

LES Simulation of Turbulent Supercritical CO₂ Heat Transfer in Microchannels

Mahdi Nabil
Graduate Research Assistant, Department
of Mechanical and Nuclear Engineering
The Pennsylvania State University
University Park, PA

Alexander S Rattner
Assistant Professor, Department of
Mechanical and Nuclear Engineering
The Pennsylvania State University
University Park, PA

ABSTRACT

Although supercritical CO₂ (sCO₂) heat transfer has been employed in industrial process since the 1960s, the underlying transport phenomenon in high-flux microscale geometries, as could be employed in concentrating solar receivers, is poorly understood. To date, nearly all experimental studies and simulations of supercritical convective heat transfer have focused on large diameter vertical channel and tube bundle flows, which may differ dramatically from microscale supercritical convection. Computational studies have primarily employed Reynolds averaged (RANS) turbulence modeling approaches, which may not capture effects from the sharply varying property trends of supercritical fluids. In this study, large eddy simulation (LES) turbulence modeling techniques are employed to study heat transfer characteristics of sCO₂ in microscale heat exchangers. The simulation geometry consists of a microchannel of 750 μm × 737 μm cross-section and 5 mm length, heated from all four sides. Simulation cases are evaluated at reduced pressure $P_r = 1.1$, mass flux $G = 1000 \text{ kg m}^{-2} \text{ s}^{-1}$, heat flux $q'' = 1.7 - 8.9 \text{ W cm}^{-2}$, and varying inlet temperature: 20 – 100°C. Computational results reveal thermal transport mechanisms specific to microscale sCO₂ flows. Results have been compared with available supercritical convection correlations [1–3] to identify the most applicable heat transfer models for engineering of microchannel sCO₂ heat exchangers.

INTRODUCTION

High heat flux thermal management technologies are critical enabling components of many engineering systems, including microelectronic devices [4,5] and solar-thermal power production [6]. Existing cooling approaches based on single-phase liquid or two-phase boiling convective heat transfer are not sufficient to meet emerging thermal management needs, such as heat fluxes $\geq 150 \text{ W cm}^{-2}$ for solar thermal power receivers [7]. Supercritical Brayton cycles have emerged as a national strategic focus for highly efficient solar thermal, geothermal, nuclear, and clean fossil energy systems [8]. These systems are capable of using high temperature solar-thermal heat more efficiently than conventional steam cycle power plants, and are more compact than equivalent steam power plants [9].

sCO₂ heat transfer has been employed in industrial process since the 1960s [10], initially for power engineering applications. However, transport behavior has only been characterized empirically and for narrow operating ranges. Prior experiments with sCO₂ [11–14] have focused on large diameter ($4.08 < D < 22.7 \text{ mm}$), uniformly heated circular tubes at low heat fluxes ($0.05 < q'' < 330 \text{ W cm}^{-2}$). Lumped wall-to-bulk property difference correction factors have been developed for plain large-diameter channel flow at low heat fluxes [11,15–17]. Some experimental heat transfer investigations have been performed in compact flow geometries, but these have been limited primarily to low-flux [18–20] heat rejection applications relevant to the

HVAC&R industry [21–23] (*i.e.*, supercritical gas coolers in transcritical refrigeration cycles). In such components energy is removed from the boundary layer, and the flow physics are expected to be significantly different than in heat acquisition. Thus, it is difficult to apply insights from supercritical cooling to heating applications. No data exists for the range of diameters ($D_H < 1$ mm) and high heat fluxes required to enable new applications in high-flux power production and electronics cooling. Therefore, the aim of this work is to elucidate the underlying transport processes and investigate the effects of individual parameters on microscale supercritical heat transfer phenomena.

Advances in computational resources and Reynolds-Averaged (RANS) turbulence modeling techniques led to increased activity in supercritical convection simulations in the 1990s and 2000s. These studies were motivated by applications in supercritical power cycles, and thus focused on moderate heat flux ($< 100 \text{ W cm}^{-2}$) water and CO_2 flows in large hydraulic diameter vertical tubes and rod bundles. Almost all such studies employed two-equation RANS turbulence models, primarily $k - \varepsilon$ [24,20,25] and $k - \omega$ [26,27] based formulations. Nearly all such studies employed steady 2-D simulations, which cannot capture key supercritical phenomena such as intrinsic pulsations identified by Bishop et al. [28] and mixed forced and free convection (*i.e.*, pseudo-boiling). In response to these limitations and discrepancies between existing RANS-based turbulence modeling studies of supercritical heat transfer, a number of investigators have recommended and performed 3D unsteady turbulence resolving simulations of supercritical flow heat transfer [29–33]. To the best of our knowledge, the only available numerical study on supercritical heat transfer at the microchannel scale was been conducted by Asinari [34], using $k - \varepsilon$ RANS formulation, which cannot resolve unsteady 3D complex turbulent structures. Detailed turbulence resolving simulations are therefore needed to advance understanding of supercritical fluid heat transfer in microchannels, and inform the selection of engineering heat transfer correlations for these conditions.

In the present investigation, high resolution large eddy simulations (LES) are performed of sCO_2 flows in microchannels at high mass fluxes ($G = 1000 \text{ kg m}^{-2}\text{s}^{-1}$) ($G = 1000 \text{ W m}^{-2}$) and moderate heat fluxes ($q'' = 1.7 - 8.9 \text{ W cm}^{-2}$). This represents the first step in a simulation campaign that will approach much higher heat fluxes. Results are used to assess the applicability of heat transfer correlations for these conditions.

SIMULATION APPROACH

The corresponding simulation geometry consists of a single microchannel test section of $750 \mu\text{m} \times 737 \mu\text{m}$ cross section, and 5 mm length. The schematic of the simulation geometry is represented in Fig. 1, and all the corresponding dimensions are listed in Table 1, below. The flow is heated from all four sides with uniform constant temperature.

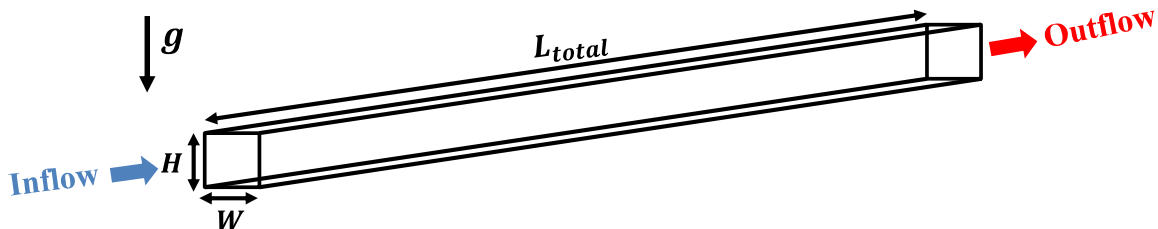


Figure 1. Schematic of the simulation geometry

Table 1. Dimensions of the simulated microchannel

Section	Size
Channel Width (W)	750.02 μm
Channel Height (H)	737.32 μm
Total Length (L_{total})	5 mm

The governing continuity, momentum, and energy equations are summarized as follows for the implicitly filtered mean velocity (u), pressure (p), and enthalpy (h) fields.

$$\frac{\partial \rho}{\partial t} + \frac{\partial}{\partial x_i} (\rho u_i) = 0 \quad (1)$$

$$\frac{\partial (\rho u_i)}{\partial t} + \frac{\partial}{\partial x_j} (\rho u_j u_i) = -\frac{\partial p}{\partial x_i} + \frac{\partial}{\partial x_j} \left[(\mu + \mu_{SGS}) \frac{\partial u_i}{\partial x_j} \right] + \rho g_i \quad (2)$$

$$\frac{\partial (\rho h)}{\partial t} + \frac{\partial}{\partial x_i} (\rho u_i h) = \frac{\partial}{\partial x_j} \left[(\alpha + \alpha_{SGS}) \frac{\partial h_i}{\partial x_j} \right] \quad (3)$$

Here, μ_{SGS} and α_{SGS} represent the LES turbulence model contributions to momentum and thermal energy transport, respectively, and stand for modeled sub-grid scale (SGS) eddy effects. Fluid thermophysical properties (ρ, c_p, μ, k) are evaluated at each time step, using explicit formulations (*i.e.*, Peng-Robinson equation of state [35]) for sCO₂ density and appropriate correlations for other fluid properties. Curve fits were developed for specific heat (c_p), dynamic viscosity (μ), and Prandtl number (Pr) for the considered reduced pressures of $P_r = 1.1$. The average absolute deviations of the fits to property values for c_p, μ , and Pr [36,37] are less than 5%, 1%, and 2%, respectively.

A velocity-pressure-enthalpy coupled unsteady compressible flow solver in OpenFOAM v1612+ [38] is employed (*buoyantPimpleFoam*). Low Mach number behavior is assumed, as in most prior sCO₂ simulation studies, such as the DNS study of Bae *et al.* [29]. The coupled momentum and pressure equations are solved with the PIMPLE algorithm, which is a combination of SIMPLE (Semi-Implicit Method for Pressure-Linked equations) [39] and PISO (Pressure Implicit Splitting Operator) [40] algorithms. The wall-adapting local eddy-viscosity (WALE) LES model [41] is used to model subgrid-scale eddy viscosity and diffusivity.

A second order implicit scheme is adopted for time discretization. Cubic interpolation is used for gradient terms (third order). Second order linear interpolation schemes are used for the divergence and Laplacian terms. Overall, this approach should yield second order accuracy for all time and spatial terms. Relevant LES studies in the literature were consulted to design the mesh structure in the computational domain [42,43]. Therefore, all the simulation test cases are designed such that the mesh near the wall region is sufficiently resolved (first cell $y^+ = 0.33$). Uniform cell size is used in the flow direction.

Constant temperature boundary condition were applied to all walls. An advective temperature boundary condition was employed for the outflow. The inflow temperature field was specified with a turbulent law of the wall profile. No-slip velocity boundary conditions were imposed on all the channel walls. A mapped velocity boundary condition was imposed at the inlet which maps the velocity field from 4 mm downstream to the inlet face. This essentially results in a fully developed turbulent velocity field throughout the domain. A *generic 0-gradient velocity boundary condition* (inletOutlet) was selected for the flow outlet. Turbulent eddy viscosity ν_t , and

turbulent diffusivity α_t were also mapped from 4 mm downstream to the inlet, and an advective outlet boundary condition was imposed for both fields. A *fixed-zero-flux* pressure boundary condition was imposed on all the walls. Fixed-value pressure inlet and outlet boundary conditions were imposed to obtain the target mass flux of $\sim 1000 \text{ kg m}^{-2} \text{ s}^{-1}$.

RESULTS AND DISCUSSION

A representative case was selected with reduced pressure of $P_r = 1.1$, mass flux $G = 1000 \text{ kg m}^{-2} \text{ s}^{-1}$ ($Re_{D,H} = 25,360$), and inlet temperature $T_{in} = 34.9 \text{ }^\circ\text{C}$ was evaluated to verify that the meshing approach (*i.e.*, first cell $y^+ = 0.33$) yielded mesh convergence. Four mesh cases were selected and designed (Fine, Finer, XFine and XXFine). The number of mesh cells for each case is listed in Table 2. All simulations were conducted with constant temperature condition for all the wall boundaries, where $T_w - T_{f,in} = 0.8 \text{ }^\circ\text{C}$. Convergence was observed for average wall heat flux value by the XFine case (q'' is within $\pm 1.5\%$ from XXFine case), indicating that no further refinement is necessary. Based on the results from the three finest mesh resolutions, the empirical rate of convergence for average wall heat flux is greater than second order. The velocity and temperature fields from this representative case are shown in Fig. 2, below.

Table 2. Summary of results for mesh independence study

Re	Case	No. of mesh elements ($x \times y \times z$)	$q''_{avg} [\text{W m}^{-2}]$
25,360	Fine	2,744,000 (140×140×140)	13,450
	Finer	7,529,536 (196×196×196)	15,600
	XFine	20,570,824 (274×274×274)	16,880
	XXFine	56,623,104 (384×384×384)	17,100

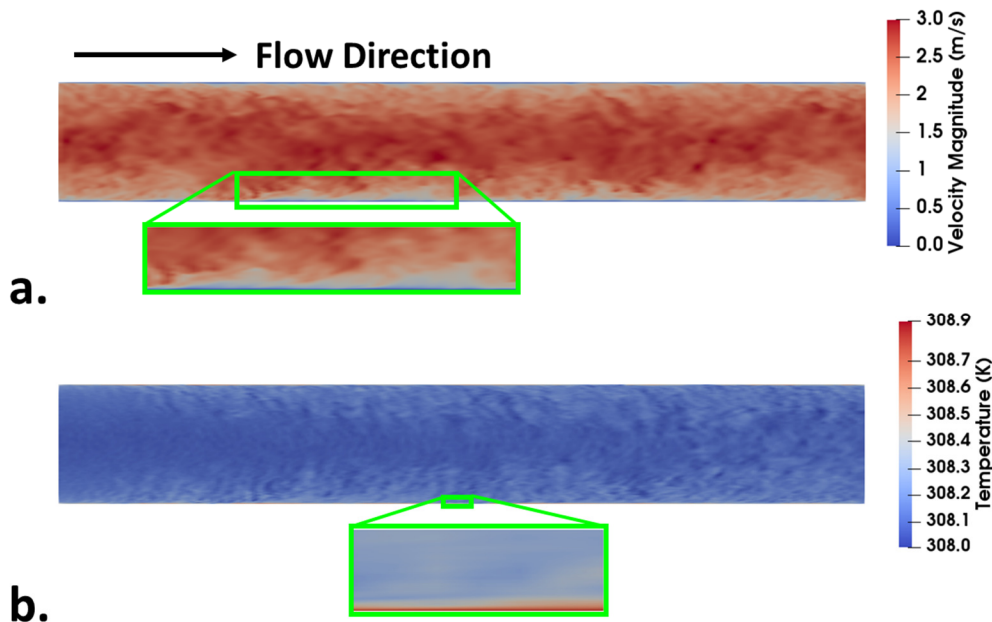


Figure 2. Simulation results for convergence test case. **a.** Cross-section velocity magnitude, with detail view of pseudo-boiling near lower wall. **b.** Channel cross-section temperature field with detail view of thermal boundary layer (lower 5% of channel).

In this study, five test cases, as shown in Table 3, were simulated. Following the method of [53] the results of three mesh resolutions were utilized to obtain Richardson-extrapolated value for average heat flux corresponding to each simulation case. Finally, the extrapolated values have been compared to available supercritical heat transfer correlations in the literature [1–3] (see Table 4).

Table 3. Specifications of selected simulation test cases. All studies at $G = 1000 \text{ kg m}^{-2} \text{ s}^{-1}$ and $Pr = 1.1$ in a $750 \text{ }\mu\text{m} \times 737 \text{ }\mu\text{m} \times 5 \text{ mm}$ channel.

Case #	Re	T_{in} [°C]	T_{wall} [°C]	$q''_{avg,extrapolated}$ [W m^{-2}]
1	11,840	20.1	26.2	$35,680 \pm 11,030$
2	15,110	29.9	32.4	$22,350 \pm 7,270$
3	25,360	34.9	35.7	$17,150 \pm 60$
4	37,470	69.9	84.7	$69,780 \pm 16,110$
5	35,870	99.9	116.7	$88,940 \pm 20,910$

Table 4. Comparison of the simulation results against predictions from supercritical correlations

Case #	Re	$q''_{avg,extrapolated}$ [W/m^2]	$q''_{Petukhov}$ [W/m^2] [1]	$q''_{Jackson}$ [W/m^2] [2]	q''_{Liao} [W/m^2] [3]
1	11,840	$35,680 \pm 11,030$	59,990	46,080	41,790
2	15,110	$22,350 \pm 7,270$	33,130	24,840	20,570
3	25,360	$17,150 \pm 60$	25,710	22,210	15,580
4	37,470	$69,780 \pm 16,110$	68,790	56,860	33,400
5	35,870	$88,940 \pm 20,910$	70,190	57,660	30,580

Out of the three considered empirical correlations from the literature [1–3], only the model of Liao and Zhao [3] was developed using data for microchannel supercritical heat transfer (tube diameter of $d = 0.7 - 2.16 \text{ mm}$). This model yields the closest agreement with simulation heat fluxes in cases 1-3 (maximum deviation of $\pm 15\%$, Table 4). Poorer agreement is found with the model of Liao and Zhao [3] at higher fluid temperatures (cases 4 and 5 with $T_{bulk} \geq 70 \text{ }^\circ\text{C}$). This may be expected, as the model of Liao and Zhao [3] only incorporated microchannel data for bulk temperatures $\leq 54^\circ\text{C}$.

Petukhov *et al.* [1] studied supercritical heat transfer in a tube with fixed diameter $D = 6.7 \text{ mm}$, $2 \times 10^4 < Re < 8.6 \times 10^5$, and $0.85 < Pr < 65$. Jackson and Hall [2] collected data from various sources, but no specific range of applicability was recommended for their correlation. The model of Petukhov *et al.* [1] results in closer agreement for heat flux with these microchannel simulations (maximum deviation of $\pm 22\%$).

At these higher fluid temperatures, sCO₂ is outside of the pseudocritical regime, and scale dependent mixed convection and boundary layer effects may be less significant. This may explain why closer agreement is obtained with larger channel diameter-based models than at lower fluid temperatures. However, there is not yet sufficient data to provide general recommendations for microchannel sCO₂ heat transfer correlations at high fluid temperatures.

The authors aim to expand the test case studies to investigate a full range of reduced pressure, wall heat flux, and the individual role of thermo-physical properties on supercritical heat transfer. The final objective is to inform new heat transfer correlations for microchannel supercritical heat transfer that incorporate highly resolved flow and temperature field data.

REFERENCES

- [1] Petukhov, B. S., Krasnoschekov, E. A., and Protopopov, V. S., 1961, "An investigation of heat transfer to fluids flowing in pipes under supercritical conditions," 1961 Int. Heat Transf. Conf., pp. 569–578.
- [2] Jackson, J. D., and Hall, W. B., 1979, "Forced convection heat transfer to fluids at supercritical pressure," *Turbul. Forced Convect. Channels Bundles Theory Appl. to Heat Exch. Nucl. React.*, pp. 563–611.
- [3] Liao, S. M., and Zhao, T. S., 2002, "An experimental investigation of convection heat transfer to supercritical carbon dioxide in miniature tubes," *Int. J. Heat Mass Transf.*, **45**(25), pp. 5025–5034.
- [4] Lin, S., Sefiane, K., and Christy, J. R. E., 2002, "Prospects of confined flow boiling in thermal management of microsystems," *Appl. Therm. Eng.*, **22**(7), pp. 825–837.
- [5] Kandlikar, S. G., and Grande, W. J., 2004, "Evaluation of Single Phase Flow in Microchannels for High Heat Flux Chip Cooling—Thermohydraulic Performance Enhancement and Fabrication Technology," *Heat Transf. Eng.*, **25**(8), pp. 5–16.
- [6] Zada, K. R., Drost, M. K., and Fronk, B. M., 2015, "Application of Microscale Devices for Megawatt Scale Concentrating Solar Power Plants," 2015 ASME International Mechanical Engineering Congress and Exposition, ASME, Houston, TX, USA.
- [7] Sargent & Lundy, 2003, "Assessment of Parabolic Trough and Power Tower Solar Technology Cost and Performance Forecasts Assessment of Parabolic Trough and Power Tower Solar Technology Cost and Performance Forecasts," Rep. No. NREL/SR-550-34440, (October), p. 47.
- [8] Iverson, B. D., Conboy, T. M., Pasch, J. J., and Kruiuzenga, A. M., 2013, "Supercritical CO₂ Brayton cycles for solar-thermal energy," *Appl. Energy*, **111**, pp. 957–970.
- [9] Turchi, C. S., Ma, Z., Neises, T. W., and Wagner, M. J., 2013, "Thermodynamic Study of Advanced Supercritical Carbon Dioxide Power Cycles for Concentrating Solar Power Systems," *ASME J. Sol. Energ.*, **135**(4), pp. 1–7.
- [10] Piore, I. L., and Duffey, R. B., 2007, "Heat Transfer and Hydraulic Resistance at Supercritical Pressures in Power Engineering Applications," ASME.

- [11] Krasnoshchekov, E. A., and Protopopov, V. S., 1966, "Experimental study of heat exchange in carbon dioxide in the supercritical range at high temperature drops(Heat transfer in turbulent carbon dioxide pipeflow at supercritical region)," *High Temp.*, **4**, pp. 375–382.
- [12] Bringer, R. P., and Smith, J. M., 1957, "Heat transfer in the critical region," *AIChE J.*, **3**(1), pp. 49–55.
- [13] Wood, R. D., and Smith, J. M., 1964, "Heat transfer in the critical region—temperature and velocity profiles in turbulent flow," *AIChE J.*, **10**(2), pp. 180–186.
- [14] Tanaka, H., Nishiwaki, N., and Hirata, M., 1967, "Turbulent heat transfer to supercritical carbon dioxide," *Semi-International Symposium, JSME*, Tokyo.
- [15] Swenson, H. S., Carver, J. R., and Kakarala, C. R. d, 1965, "Heat transfer to supercritical water in smooth-bore tubes," *J. Heat Transfer*, **87**(4), pp. 477–483.
- [16] Yamagata, K., Nishikawa, K., Hasegawa, S., Fujii, T., and Yoshida, S., 1972, "Forced convective heat transfer to supercritical water flowing in tubes," *Int. J. Heat Mass Transf.*, **15**(12), pp. 2575–2593.
- [17] Jackson, J. D., 2002, "Consideration of the heat transfer properties of supercritical pressure water in connection with the cooling of advanced nuclear reactors," *The 13th pacific basin nuclear conference. Abstracts*.
- [18] Liao, S. M., and Zhao, T. S., 2002, "Measurements of Heat Transfer Coefficients From Supercritical Carbon Dioxide Flowing in Horizontal Mini/Micro Channels," *J. Heat Transfer*, **124**(3), p. 413.
- [19] Pitla, S. S., Robinson, D. M., Groll, E. A., and Ramadhyani, S., 1998, "Heat transfer from supercritical carbon dioxide in tube flow: a critical review," *Hvac&R Res.*, **4**(3), pp. 281–301.
- [20] Dang, C., and Hihara, E., 2004, "In-tube cooling heat transfer of supercritical carbon dioxide. Part 1. Experimental measurement," *Int. J. Refrig.*, **27**(7), pp. 736–747.
- [21] Groll, E. A., and Kim, J.-H., 2007, "Review of recent advances toward transcritical CO₂ cycle technology," *Hvac&R Res.*, **13**(3), pp. 499–520.
- [22] Fronk, B. M., and Garimella, S., 2011, "Water-coupled carbon dioxide microchannel gas cooler for heat pump water heaters: Part I-Experiments," *Int. J. Refrig.*, **34**(1), pp. 7–16.
- [23] Fronk, B. M., and Garimella, S., 2011, "Water-coupled carbon dioxide microchannel gas cooler for heat pump water heaters: Part II-Model development and validation," *Int. J. Refrig.*, **34**(1), pp. 17–28.
- [24] Shiralkar, B., and Griffith, P., 1970, "The effect of swirl, inlet conditions, flow direction, and tube diameter on the heat transfer to fluids at supercritical pressure," *J. Heat Transfer*, **92**(3), pp. 465–471.
- [25] Bellinghausen, R., and Renz, U., 1990, "Pseudocritical heat transfer inside vertical

- tubes,” *Chem. Eng. Process. Process Intensif.*, **28**(3), pp. 183–186.
- [26] He, S., Jiang, P.-X., Xu, Y.-J., Shi, R.-F., Kim, W. S., and Jackson, J. D., 2005, “A computational study of convection heat transfer to CO₂ at supercritical pressures in a vertical mini tube,” *Int. J. Therm. Sci.*, **44**(6), pp. 521–530.
- [27] Cheng, X., Kuang, B., and Yang, Y. H., 2007, “Numerical analysis of heat transfer in supercritical water cooled flow channels,” *Nucl. Eng. Des.*, **237**(3), pp. 240–252.
- [28] Bishop, A. A., Sandberg, R. O., and Tong, L. S., 1964, *Forced-convection heat transfer to water at near-critical temperatures and supercritical pressures*, Westinghouse Electric Corp., Pittsburgh, Pa. Atomic Power Div.
- [29] Bae, J. H., Yoo, J. Y., and Choi, H., 2005, “Direct numerical simulation of turbulent supercritical flows with heat transfer,” *Phys. Fluids*, **17**(10).
- [30] Bae, J. H., Yoo, J. Y., and McEligot, D. M., 2008, “Direct numerical simulation of heated CO₂ flows at supercritical pressure in a vertical annulus at Re= 8900,” *Phys. Fluids*, **20**(5), p. 55108.
- [31] Yoo, J. Y., 2013, “The turbulent flows of supercritical fluids with heat transfer,” *Annu. Rev. Fluid Mech.*, **45**(1), pp. 495–525.
- [32] Azih, C., Brinkerhoff, J. R., and Yaras, M. I., 2012, “Direct numerical simulation of convective heat transfer in a zero-pressure-gradient boundary layer with supercritical water,” *J. Therm. Sci.*, **21**(1), pp. 49–59.
- [33] Licht, J., Anderson, M., and Corradini, M., 2009, “Heat Transfer and Fluid Flow Characteristics in Supercritical Pressure Water,” *J. Heat Transfer*, **131**(7), p. 072502.
- [34] Asinari, P., 2005, “Numerical prediction of turbulent convective heat transfer in mini/micro channels for carbon dioxide at supercritical pressure,” *Int. J. Heat Mass Transf.*, **48**(18), pp. 3864–3879.
- [35] Peng, D.-Y., and Robinson, D. B., 1976, “A new two-constant equation of state,” *Ind. Eng. Chem. Fundam.*, **15**(1), pp. 59–64.
- [36] Fenghour, A., Wakeham, W. A., and Vesovic, V., 1998, “The viscosity of carbon dioxide,” *J. Phys. Chem. Ref. Data*, **27**(1), pp. 31–44.
- [37] Vesovic, V., Wakeham, W. A., Olchowky, G. A., Sengers, J. V., Watson, J. T. R., and Millat, J., 1990, “The transport properties of carbon dioxide,” *J. Phys. Chem. Ref. data*, **19**(3), pp. 763–808.
- [38] OpenCFD Ltd., 2016, “OpenFOAM v1612+.”
- [39] Ferziger, J. H., and Peric, M., 2012, *Computational methods for fluid dynamics*, Springer Science & Business Media.
- [40] Issa, R. I., 1982, “Solution of the Implicit Discretized Fluid Flow Equations by Operator Splitting,” Imperial College, London, UK.

- [41] Ducros, F., Nicoud, F., and Poinso, T., 1998, "Wall-adapting local eddy-viscosity models for simulations in complex geometries," Numer. Methods Fluid Dyn. VI, pp. 293–299.
- [42] Moin, P., and Kim, J., 1985, "Numerical investigation of turbulent channel flow," J. Fluid Mech., **118**, pp. 341–377.
- [43] Dong, Y. H., Lu, X. Y., and Zhuang, L. X., 2002, "An investigation of the Prandtl number effect on turbulent heat transfer in channel flows by large eddy simulation," Acta Mech., **159**, pp. 39–51.

ACKNOWLEDGEMENTS

The authors wish to acknowledge generous financial support from the U.S. National Science Foundation (grant number CBET-1604538), and computing resources from the Penn State ACI high performance computing system.

AUTHORS BIOGRAPHY



Mahdi Nabil is a PhD candidate in Mechanical Engineering at The Pennsylvania State University. He received his B.Sc. and M.Sc. degrees in Mechanical Engineering from Amirkabir University of Technology (Tehran Polytechnic) and Auburn University in 2011 and 2013, respectively. His research interests include multiphase flow heat and mass transfer, bioheat transfer, and supercritical fluid heat transfer.



Alexander S Rattner is the principal investigator of the Multiscale Thermal Fluids and Energy Lab. He is the Dorothy Quiggle Career Development assistant professor in the Department of Mechanical and Nuclear Engineering at Penn State. He received his Ph.D. in Summer 2015 from the Georgia Institute of Technology as a US Department of Energy Computational Science Graduate Fellow. His research expertise includes waste heat recovery, absorption refrigeration, high-heat-flux thermal management, power systems for planetary landers, membrane distillation, air-cooled condensers for power plants, and experimental and computational multiphase flow heat and mass transfer.